Acta Cryst. (1977). B33, 2258–2263

The Crystal Structures of Free Radical Salts and Complexes.
X. The Crystal Structure and Electrical Properties of $[1,2\text{-Di}(N\text{-benzyl-4-pyridinium})\text{ethylene}]^{2+}(7,7,8,8\text{-Tetracyanoquinodimethane})_5^{2-}$

By G. J. Ashwell,* D. D. Eley, A. Harper, A. C. Torrance, S. C. Wallwork and M. R. Willis

Department of Chemistry, University of Nottingham, Nottingham NG7 2RD, England

(*Received* 20 *December* 1976; *accepted* 22 *January* 1977)

The crystal structure, electrical conductivity and thermoelectric power of a complex of unusual stoichiometry, $[1,2\text{-di}(N\text{-benzyl-4-pyridinium})\text{ethylene}]^{2+}(7,7,8,8\text{-tetracyanoquinodimethane})_5^{2-}$, $(\text{DBzPE})^{2+}$-$(\text{TCNQ})_5^{2-}$, are reported. The complex is triclinic, space group $P\bar{1}$, with $a = 8{\cdot}043$, $b = 17{\cdot}356$, $c = 15{\cdot}209$ Å, $\alpha = 100{\cdot}96$, $\beta = 110{\cdot}10$, $\gamma = 112{\cdot}45°$, $Z = 1$. The TCNQ's stack plane-to-plane in columns such that each exocyclic $C{=}C(CN)_2$ double bond overlaps the quinonoid ring of an adjacent molecule. The electrical data indicate the onset of metallic behaviour at high temperatures.

Introduction

TCNQ salts are of interest since their electrical properties vary from insulating to metallic with room-temperature conductivities in the range 10^3 to 10^{-14} Ω^{-1} cm^{-1}. A condition for high conductivity is a parallel plane-to-plane stacking of the anions in columns, with a regular interplanar spacing of $\sim 3{\cdot}2$ Å and an exocyclic double bond to quinonoid ring overlap. It is also necessary for the longitudinal staggering of adjacent TCNQ's to be in a consistent direction throughout the stack. One form of the complex salt, $[1,2\text{-di}(N\text{-ethyl-4-pyridinium})\text{ethylene}]^{2+}(\text{TCNQ})_4^{2-}$, $(\text{DEPE})^{2+}$-$(\text{TCNQ})_4^{2-}$ I, has a high metallic conductivity of 150–2200 Ω^{-1} cm^{-1} at 300 K (Ashwell, Eley & Willis, 1976) which on cooling to 30 mK increases monotonically. In this paper we report the conductivity, thermoelectric power and crystal structure of a related dibenzyl complex. The effect of the larger quaternary group is to reduce the conductivity. However, at higher temperatures some of the metallic character is retained.

Experimental

Crystal data

$(C_{26}H_{24}N_2)(C_{12}H_4N_4)_5$, $M_r = 1385{\cdot}3$. Triclinic, $a = 8{\cdot}043\,(5)$, $b = 17{\cdot}356\,(7)$, $c = 15{\cdot}209\,(3)$ Å, $\alpha = 100{\cdot}96\,(8)$, $\beta = 110{\cdot}10\,(2)$, $\gamma = 112{\cdot}45\,(12)°$; $U = 1711{\cdot}7$ Å^3, $D_m = 1{\cdot}32\,(2)$, $Z = 1$, $D_c = 1{\cdot}344$ g cm^{-3}; $F(000) = 714$. Mo $K\alpha$($\lambda = 0{\cdot}71069$ Å), $\mu = 0{\cdot}91$ cm^{-1}. Space group $P\bar{1}$ (assumed).

Black crystals of $(\text{DBzPE})^{2+}(\text{TCNQ})_5^{2-}$ were deposited when a warm acetonitrile solution (200 ml) of TCNQ (0·2 g) and LiTCNQ (0·2 g) was added to an aqueous solution (10 ml) of 1,2-di(*N*-benzyl-4-pyridinium)ethylene dichloride (0·2 g) and allowed to cool slowly. The space group and cell dimensions were obtained initially from oscillation and Weissenberg photographs with Cu $K\alpha$ radiation. The cell constants were subsequently refined on a Hilger & Watts computer-controlled, four-circle diffractometer. Intensities were collected with a $\theta/2\theta$ scan, a scintillation counter and Mo $K\alpha$ radiation. The intensities were corrected for Lorentz and polarization factors but not for absorption.

Measurements of the electrical conductivity and thermoelectric power were carried out as reported previously (Ashwell, Eley, Willis & Woodward, 1977).

Structure determination

The structure was solved from a Patterson synthesis and refined initially by block-diagonal least squares with 3160 significant reflexions $[I > 3\sigma(I)]$. Refinement of the positional and isotropic thermal parameters of the non-hydrogen atoms, with unit weights, gave $R = 0{\cdot}127$. Positional parameters of the H atoms were calculated from the coordinates of the C atoms and confirmed by a difference synthesis. These atoms were included in the subsequent refinement in fixed positions with constant isotropic thermal parameters of 0·06 Å^2. Block-diagonal, least-squares refinement of the non-hydrogen atoms with anisotropic thermal parameters and the weighting scheme $w = 1/\{1 + [(|F_o| - A)/B]^2\}$ where $|F_o|$ is on the absolute scale, $A = 10{\cdot}5$ and $B = 17{\cdot}0$ gave a final $R = 0{\cdot}063$. Scattering factors were taken from *International Tables for X-ray Crystallography* (1974). The final positional parameters are listed in Table 1. Least-squares planes were calculated for

---

* Address for 1977: Department of Chemistry, University of Queensland, Brisbane, Qld 4067, Australia.

Table 1. *Final positional parameters* ($\times 10^4$)

The figures in parentheses indicate standard deviations.

	x	y	z		x	y	z
C(1)	1669 (5)	168 (2)	878 (3)	C(22)	−3528 (5)	3618 (2)	−1849 (3)
C(2)	−225 (5)	−4 (2)	876 (3)	C(23)	−1631 (5)	3802 (3)	−1846 (3)
C(3)	−1823 (5)	−163 (2)	33 (3)	C(24)	−21 (5)	3966 (3)	−1012 (3)
C(4)	3293 (5)	317 (2)	1736 (3)	C(25)	1478 (5)	4113 (2)	747 (3)
C(5)	5199 (6)	508 (3)	1762 (3)	C(26)	3372 (6)	4283 (3)	754 (3)
C(6)	3150 (6)	298 (3)	2642 (3)	C(27)	1377 (6)	4097 (3)	1663 (3)
N(1)	6723 (5)	653 (3)	1780 (3)	C(28)	−5182 (6)	3444 (3)	−2702 (3)
N(2)	3060 (6)	272 (3)	3366 (3)	C(29)	−7082 (6)	3243 (3)	−2715 (3)
C(7)	789 (5)	2054 (2)	357 (3)	C(30)	−5076 (6)	3432 (3)	−3620 (3)
C(8)	−1068 (5)	1885 (2)	396 (3)	N(7)	4888 (5)	4422 (3)	774 (3)
C(9)	−2726 (5)	1716 (2)	−421 (3)	N(8)	1311 (6)	4082 (3)	2395 (3)
C(10)	−2960 (5)	1701 (2)	−1358 (3)	N(9)	−8593 (6)	3076 (3)	−2717 (3)
C(11)	−838 (5)	1877 (2)	−1399 (3)	N(10)	−4976 (6)	3414 (3)	−4354 (3)
C(12)	811 (5)	2042 (2)	−583 (3)	C(31)	−499 (7)	128 (5)	5124 (4)
C(13)	2473 (5)	2211 (2)	1185 (3)	C(32)	73 (7)	2078 (3)	4108 (3)
C(14)	4330 (6)	2376 (3)	1158 (3)	C(33)	386 (7)	1401 (4)	4319 (4)
C(15)	2507 (6)	2213 (3)	2130 (3)	C(34)	−644 (8)	928 (3)	4768 (4)
C(16)	−4389 (5)	1533 (2)	−2187 (3)	C(35)	−1992 (8)	1147 (4)	4983 (4)
C(17)	−6245 (6)	1362 (3)	−2158 (3)	C(36)	−2221 (6)	1824 (3)	4764 (3)
C(18)	−4425 (6)	1527 (3)	−3130 (3)	C(37)	−1454 (7)	3066 (3)	4153 (3)
N(3)	5833 (6)	2509 (3)	1166 (3)	C(38)	−15 (7)	4203 (3)	5858 (4)
N(4)	2587 (6)	2219 (3)	2892 (3)	C(39)	1567 (9)	4974 (4)	6670 (4)
N(5)	−7728 (6)	1244 (3)	−2150 (3)	C(40)	3311 (7)	5456 (3)	6642 (4)
N(6)	−4507 (6)	1529 (3)	−3896 (3)	C(41)	3503 (7)	5205 (4)	5801 (4)
C(19)	−153 (5)	3960 (2)	−97 (3)	C(42)	1951 (7)	4433 (4)	4990 (4)
C(20)	−2045 (5)	3786 (2)	−96 (3)	C(43)	188 (6)	3915 (3)	5010 (3)
C(21)	−3642 (5)	3627 (2)	−926 (3)	N(11)	−1239 (5)	2283 (2)	4327 (2)

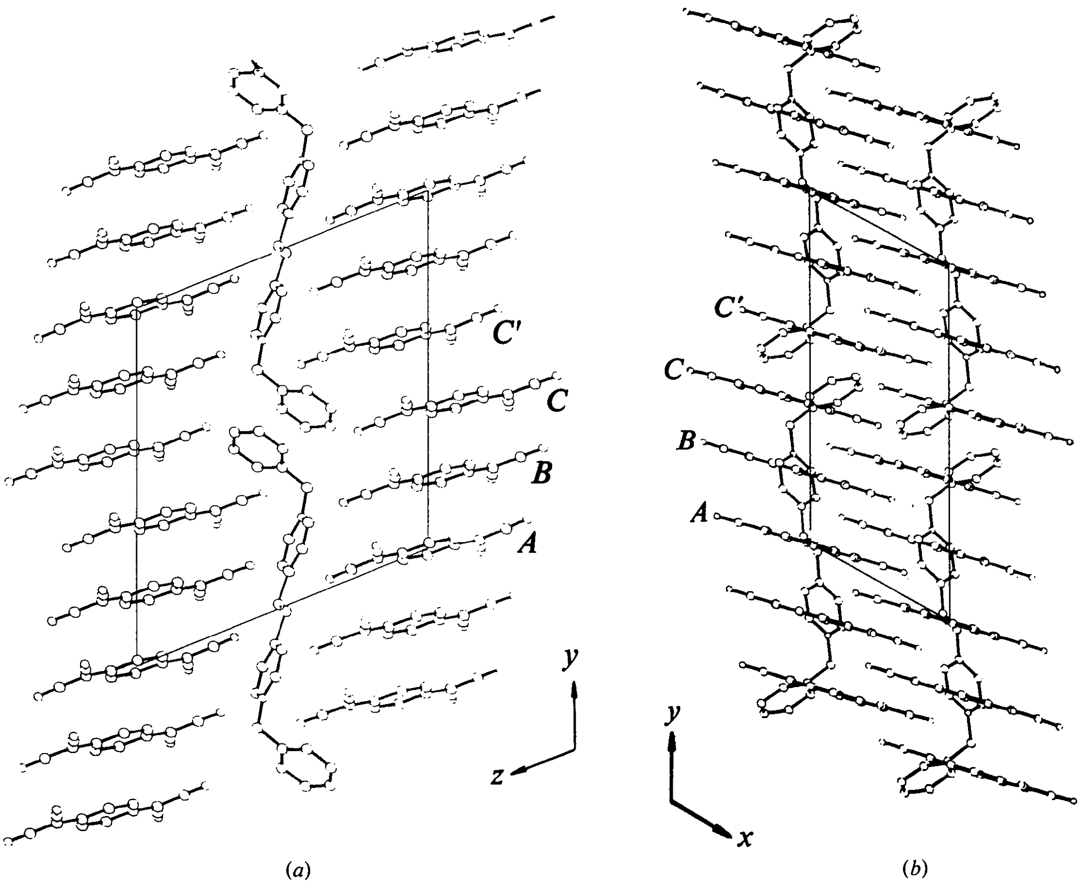

(*a*) (*b*)

Fig. 1. The crystal structure of $(\mathrm{DBzPE})^{2+}(\mathrm{TCNQ})_5^{2-}$ projected (*a*) along **a** and (*b*) along **c**.

Table 2. *Details of molecular planes (x,y,z are fractional atomic coordinates)*

TCNQ(*A*)

Equations to the planes

Molecule

$$-1{\cdot}586x + 16{\cdot}231y + 0{\cdot}211z - 0{\cdot}033 = 0$$

Quinonoid group

$$-1{\cdot}479x + 16{\cdot}280y - 0{\cdot}145z - 0{\cdot}009 = 0$$

Distances from the planes (Å)

	Molecule	Quinonoid group
C(1)	−0·006	0·005
C(2)	0·015	0·005
C(3)	−0·008	−0·005
C(4)	−0·004	−0·005
C(5)	0·004	0·024*
C(6)	0·007	−0·028*
N(1)	−0·002	0·034*
N(2)	−0·007	−0·069*

TCNQ(*B*)

Equations to the planes

Molecule

$$-1{\cdot}506x + 16{\cdot}292y - 0{\cdot}127z - 3{\cdot}205 = 0$$

Quinonoid group

$$-1{\cdot}507x + 16{\cdot}330y - 0{\cdot}240z - 3{\cdot}221 = 0$$

Distances from the planes (Å)

	Molecule	Quinonoid group
C(7)	0·018	0·005
C(8)	0·021	0·007
C(9)	0·007	0·002
C(10)	−0·013	−0·007
C(11)	−0·003	0·004
C(12)	0·008	0·005
C(13)	0·010	−0·012
C(14)	−0·000	−0·022*
C(15)	−0·004	−0·036*
C(16)	−0·018	−0·004
C(17)	−0·018	−0·004*
C(18)	−0·011	0·014
N(3)	−0·010	−0·031*
N(4)	−0·016	−0·057*
N(5)	0·013	0·027*
N(6)	0·015	0·048*

TCNQ(*C*)

Equations to the planes

Molecule

$$-1{\cdot}583x + 16{\cdot}349y - 0{\cdot}141z - 6{\cdot}474 = 0$$

Quinonoid group

$$-1{\cdot}534x + 16{\cdot}340y - 0{\cdot}212z - 6{\cdot}495 = 0$$

Distances from the planes (Å)

	Molecule	Quinonoid group
C(19)	0·026	0·001
C(20)	0·041	0·007
C(21)	0·046	0·010
C(22)	0·026	−0·003
C(23)	0·026	0·007
C(24)	0·028	0·010
C(25)	0·006	−0·017
C(26)	−0·016	−0·030*
C(27)	−0·017	−0·047*
C(28)	0·015	−0·015
C(29)	−0·012	−0·052*
C(30)	−0·008	−0·032*
N(7)	−0·029	−0·036*
N(8)	−0·042	−0·077*
N(9)	−0·046	−0·093*
N(10)	−0·043	−0·061*

Pyridinium ring

Equation to the plane

$$2{\cdot}087x + 3{\cdot}740y + 8{\cdot}834z - 4{\cdot}421 = 0$$

Distances from the plane (Å)

C(32)	0·001	C(35)	−0·006
C(33)	−0·001	C(36)	0·006
C(34)	0·003	N(11)	−0·003

Benzene ring

Equation to the plane

$$-4{\cdot}510x + 15{\cdot}502y - 6{\cdot}020z - 2{\cdot}984 = 0$$

Distances from the plane (Å)

C(38)	0·012	C(41)	0·013
C(39)	0·005	C(42)	0·004
C(40)	−0·018	C(43)	−0·016

* Denotes atoms not defining the plane.

each of the TCNQ moieties and the phenyl and pyridinium rings of the cation; the results are summarized in Table 2.*

Discussion

Description of the structure

The structure of (DBzPE)$^{2+}$(TCNQ)$_5^{2-}$ projected along **a** and **c** is shown in Fig. 1. The TCNQ molecules are stacked plane-to-plane in columns along **b** with mean interplanar spacings of 3·20 ± 0·03 (3·22 ± 0·01), 3·23 ± 0·04 (3·27 ± 0·01) and 3·40 ± 0·03 (3·40 ± 0·01) Å between *AB*, *BC* and *CC'* respectively. The dihedral angles between *AB* and *BC* are 1·3 (0·5) and 0·6 (0·2)° respectively. The figures in parentheses indicate the mean distances and angles between the quinonoid rings and differ because of the slight out-of-plane distortions of the C(CN)$_2$ groups. Other short intermolecular distances are listed in Table 3.

Within the columns, the TCNQ's are grouped in

---

* Lists of structure factors and anisotropic thermal parameters have been deposited with the British Library Lending Division as Supplementary Publication No. SUP 32448 (36 pp.). Copies may be obtained through The Executive Secretary, International Union of Crystallography, 13 White Friars, Chester CH1 1NZ, England.

fives with an exocyclic double bond to quinonoid ring overlap of adjacent molecules. Within pentads the staggering of molecules is in the same direction. Between pentads, *i.e.* between TCNQ(*C*) and TCNQ(*C′*), the direction of staggering is reversed (Fig. 1) but the type of overlap remains the same (Fig. 2).

The dimensions of the three crystallographically independent types of TCNQ moiety are shown in Fig. 3 and the averaged lengths of chemically similar bonds are summarized in Table 4. The average values for TCNQ(*A*), TCNQ(*B*) and TCNQ(*C*) are, within experimental error, identical and are similar to those observed for TCNQ$^{1/2-}$ (Ashwell, Eley, Wallwork & Willis, 1975). Some dimensions of TCNQ(*C*) are similar to those for TCNQ° but this is not considered to be strong evidence for charge localization. The negative charge is therefore more likely to be evenly distributed, on average, within the pentad, with a mean charge of 0·4− on each TCNQ.

The dimensions of the cation (Fig. 3) are generally in close agreement with values reported for *N*,*N′*-dibenzyl-4,4′-bipyridylium(TCNQ)$_4$ (Sundaresan &

Table 3. *Short intermolecular contacts* (Å)

The standard deviations are 0·004–0·005 Å.

TCNQ(*A*)–TCNQ(*B*)	
C(1^{i})–C(7^{i})	3·343
C(1^{i})–C(13^{i})	3·260
C(1^{i})–C(15^{i})	3·377
C(2^{i})–C(12^{i})	3·304
C(2^{i})–C(15^{i})	3·338
C(3^{i})–C(8^{i})	3·267
C(3^{i})–C(14^{i})	3·322
C(4^{i})–C(10^{i})	3·251
C(4^{i})–C(11^{i})	3·388
C(5^{i})–C(9^{i})	3·371
C(5^{i})–C(10^{i})	3·388
C(6^{i})–C(11^{i})	3·284
Inter-stack	
C(9^{i})–N(3^{ii})	3·307
C(12^{i})–N(5^{iii})	3·301
C(20^{i})–C(24^{iv})	3·383
N(7^{i})–N(7^{v})	3·377

TCNQ(*B*)–TCNQ(*C*)	
C(7^{i})–C(25^{i})	3·300
C(8^{i})–C(27^{i})	3·337
C(9^{i})–C(20^{i})	3·329
C(10^{i})–C(19^{i})	3·399
C(11^{i})–C(24^{i})	3·321
C(12^{i})–C(26^{i})	3·391
C(16^{i})–C(22^{i})	3·311
TCNQ cation	
N(1^{i})–C(32^{iii})	3·307
N(2^{i})–C(35^{iii})	3·380
N(2^{i})–C(36^{iii})	3·263
N(4^{i})–C(32^{i})	3·153
N(6^{i})–C(35^{vi})	3·225
N(6^{i})–C(36^{vi})	3·170
N(9^{i})–C(38^{vii})	3·384
N(10^{i})–C(32^{vii})	3·344

Superscripts correspond to equivalent positions as follows:

(i)	x	y,	z	(iv)	$\bar{x}$,	$1-y$,	$\bar{z}$
(ii)	$x-1$,	y,	z	(v)	$1-x$,	$1-y$,	$\bar{z}$
(iii)	$x+1$,	y,	z	(vi)	x,	y,	$z-1$
				(vii)	$x-1$,	y,	$z-1$

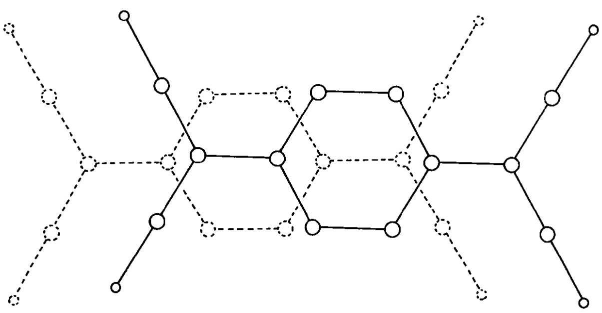

Fig. 2. TCNQ molecular overlap.

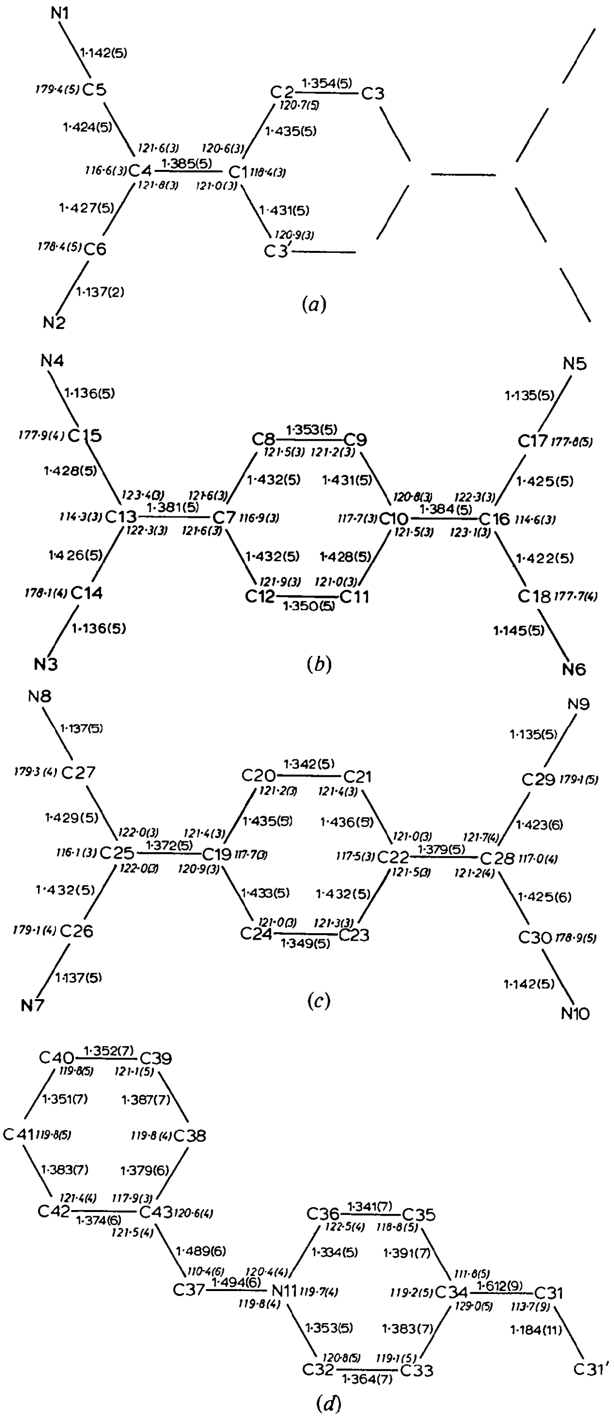

Fig. 3. Bond lengths (Å) and angles (°) with their standard deviations in parentheses for (*a*) TCNQ(*A*), (*b*) TCNQ(*B*), (*c*) TCNQ(*C*) and (*d*) the cation.

Table 4. *Comparison of mean bond lengths* (Å, *uncorrected for libration*)

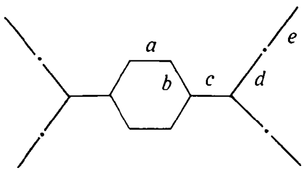

Bond	*a*	*b*	*c*	*d*	*e*
*TCNQ°	1·346	1·448	1·374	1·440	1·138
†TCNQ$^-$	1·362	1·424	1·413	1·417	1·149
†TCNQ$^{1/2-}$	1·355	1·433	1·396	1·424	1·145
TCNQ(*A*)	1·354	1·433	1·385	1·426	1·140
TCNQ(*B*)	1·352	1·431	1·383	1·425	1·138
TCNQ(*C*)	1·346	1·434	1·376	1·427	1·138
Mean of *A*,*B*,*C*	1·350 (5)	1·433 (2)	1·380 (5)	1·426 (3)	1·138 (3)

* Long, Sparks & Trueblood (1965).
† Ashwell, Eley, Wallwork & Willis (1975).

Wallwork, 1972), 1,2-di(*N*-ethyl-4-pyridinium)-ethylene(TCNQ)$_4$ (Ashwell, Eley, Fleming, Wallwork & Willis, 1976) and 1,2-di(*N*-ethyl-4-pyridinium)-ethane(TCNQ)$_4$ (Ashwell, Eley, Wallwork, Willis, Welch & Woodward, 1977). The C(31)–C(31′) and C(31)–C(34) distances, however, are clearly erroneous. Immediately prior to the final refinement, C(31) was shifted to a more sensible position, calculated on the basis of expected bond lengths and angles, but on refining it reverted to almost the same erroneous position. The angle between the phenyl and pyridinium rings is 76·1°. The angles that these planes make with TCNQ(*A*) are 47·4 and 57·0°, with TCNQ(*B*) 46·9 and 57·7° and with TCNQ(*C*) 46·3 and 58·2° respectively.

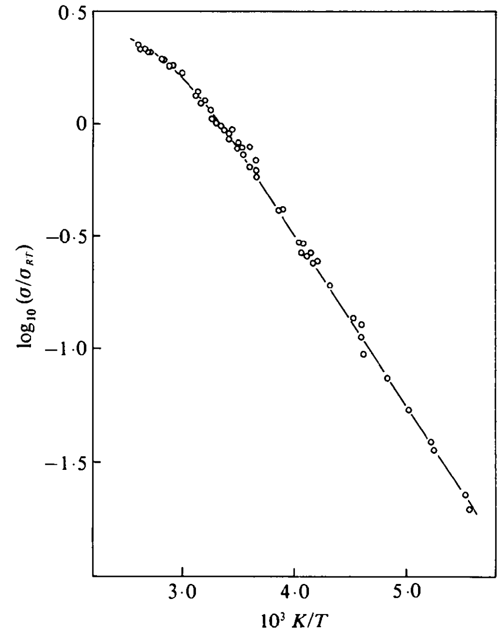

Fig. 4. Temperature dependence of the normalized conductivity of (DBzPE)$^{2+}$(TCNQ)$_5^{2-}$.

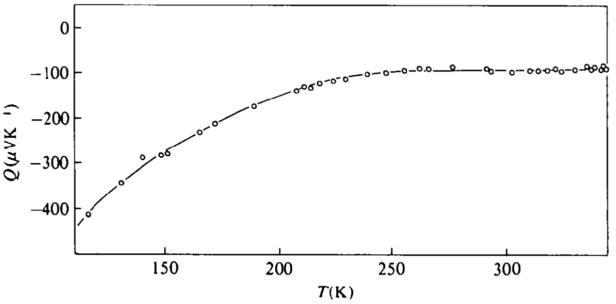

Fig. 5. Temperature dependence of the thermoelectric power of (DBzPE)$^{2+}$(TCNQ)$_5^{2-}$.

Electrical properties

The temperature dependence of the normalized conductivity of (DBzPE)$^{2+}$(TCNQ)$_5^{2-}$ is shown in Fig. 4. The crystal conductivity along the long crystal axis, *b*, *i.e.* along the TCNQ stacking direction, is in the range 0·1 to 1 Ω^{-1} cm^{-1} at 300 K with a corresponding activation energy of 0·14 ± 0·02 eV. Above 300 K, deviation from linearity of the log *σ v.* 10^3 K/*T* plot may indicate the onset of metallic behaviour. However, the metal-to-insulator transition is unobtainable owing to the sublimation of TCNQ and the subsequent decomposition of the complex at higher temperatures.

The conductivity of 0·1 to 1 Ω^{-1} cm^{-1} reflects the favourable exocyclic double bond to quinonoid ring overlap of adjacent anions and the relatively short separations within the pentads. However, a greater separation of 3·40 ± 0·03 Å and a change in the direction of staggering between pentads limits the conductivity and suppresses the metallic state at normal temperatures.

The temperature dependence of the thermoelectric power of (DBzPE)$^{2+}$(TCNQ)$_5^{2-}$ is shown in Fig. 5; above 250 K the thermoelectric EMF remains constant at −85 ± 10 μV K^{-1}. Such behaviour is common to highly conducting TCNQ complex salts of nitrogen heterocyclic bases (Shchegolev, 1972) and has been discussed by Chaikin & Beni (1976). For a system of localized carriers with strong on-site electron–electron Coulomb repulsion, the thermoelectric power (*Q*) is given by

$$Q = -k/e \ln[2(1-\rho)/\rho] \qquad (1)$$

where ρ is the ratio of carriers to sites. In the highly conducting complexes where $\rho = \frac{1}{2}$ (Beni, Kwak & Chaikin, 1975), the experimental thermoelectric EMF's are consistent with the theoretical value of −59·8 μV K^{-1} calculated from (1). Here we report a complex of unusual stoichiometry whose thermoelectric power is governed by the Chaikin & Beni expression. The experimental thermoelectric EMF of −85 ± 10 μV K^{-1} for $T > 250$ K is in good agreement with the theoretical value of −94·8 μV K^{-1} obtained by substituting $\rho = 0{\cdot}4$ in (1). The data therefore suggest that a narrow band model, with correlated carrier motion, is appropriate. This is not inconsistent with the structural data, which are best interpreted in terms of a fairly even distribution of electrons over the pentad. Such a distribution could result from either true electron delocalization or from a random distribution of localized charges. The evidence of correlated carrier motion from the thermoelectric power results seems to indicate some degree of localization.

We thank Professor T. J. King for assistance with the diffractometry and the computing and the SRC for contributing towards the cost of the diffractometer.

References

Ashwell, G. J., Eley, D. D., Fleming, R. J., Wallwork, S. C. & Willis, M. R. (1976). *Acta Cryst.* B**32**, 2948–2952.

Ashwell, G. J., Eley, D. D., Wallwork, S. C. & Willis, M. R. (1975). *Proc. Roy. Soc.* A**343**, 461–475.

Ashwell, G. J., Eley, D. D., Wallwork, S. C., Willis, M. R., Welch, G. D. & Woodward, J. (1977). *Acta Cryst.* B**33**, 2252–2257.

Ashwell, G. J., Eley, D. D. & Willis, M. R. (1976). *Nature, Lond.* **259**, 201–202.

Ashwell, G. J., Eley, D. D., Willis, M. R. & Woodward, J. (1977). *Phys. Stat. Sol.* In the press.

Beni, G., Kwak, J. F. & Chaikin, P. M. (1975). *Solid State Commun.* **17**, 1549.

Chaikin, P. M. & Beni, G. (1976). *Phys. Rev.* B**13**, 647.

International Tables for X-ray Crystallography (1974). Vol. IV. Birmingham: Kynoch Press.

Long, R. E., Sparks, R. A. & Trueblood, K. N. (1965). *Acta Cryst.* **18**, 932–939.

Shchegolev, I. F. (1972). *Phys. Stat. Sol.* **12**, 9–45.

Sundaresan, T. & Wallwork, S. C. (1972). *Acta Cryst.* B**28**, 2474–2480.